

Supplementary Information (SI)

**TiC<sub>2</sub>: A New Two Dimensional Sheet beyond MXenes**

Tianshan Zhao,<sup>a,b</sup> Shunhong Zhang,<sup>a,b</sup> Yaguang Guo,<sup>a,b</sup> and Qian Wang<sup>\*a,b</sup>

<sup>a</sup>Center for Applied Physics and Technology, College of Engineering, Peking University, Beijing 100871, China

<sup>b</sup>IFSA Collaborative Innovation Center, and Key Laboratory of High Energy Density Physics Simulation, Ministry of Education, Beijing 100871, China

E-mail: [qianwang2@pku.edu.cn](mailto:qianwang2@pku.edu.cn)

**1. Candidate structures of C<sub>2</sub> containing TiC<sub>2</sub>**

By depositing C<sub>2</sub> dimers on the surface of a monolayer triangular Ti lattice, we obtain three candidate structures of the 2D TiC<sub>2</sub> sheet.

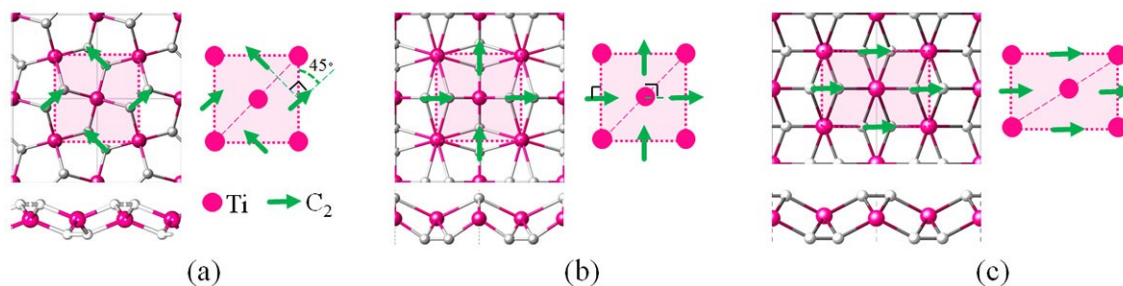


**Fig. S1** C<sub>2</sub> dimers inserted at different positions and with different orientations on the surface of a triangular Ti lattice. (a) C<sub>2</sub> dimers bind to Ti atoms in EOC mode, and perpendicular to the nearest neighboring C<sub>2</sub> dimers; (b) C<sub>2</sub> dimers bind to Ti atoms in both SOC and EOC modes, and perpendicular to the near neighboring C<sub>2</sub> dimers; (c) C<sub>2</sub> dimers bind to Ti atoms in both SOC and EOC modes, but are all parallelly aligned.

## 2. Stability relative to the 2D TiC<sub>2</sub> isomeric structures

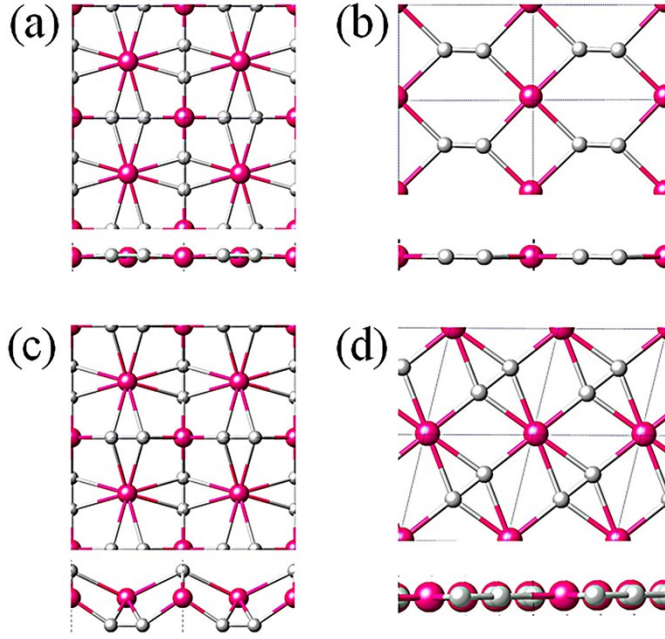


**Fig. S2** Two energetically low-lying structural isomers of TiC<sub>2</sub> containing C<sub>2</sub> units. (a) and (b) are the initial structures; (c) and (d) are the corresponding optimized structures, respectively.

## 3. Stability relative to other Ti-C compounds

For comparison, we calculated the cohesive energy of TiC<sub>2</sub>, Ti<sub>3</sub>C<sub>2</sub> (MXene), bulk TiC, and some other Ti-C binary compounds. To gauge the relative stability of a compound with the composition of Ti<sub>x</sub>C<sub>1-x</sub>, using the method described by Zhang et al.<sup>1</sup>, we define its molar formation energy  $\delta F$  as

$$\delta F(\text{Ti}_x\text{C}_{1-x}) = E_{\text{coh}}(\text{Ti}_x\text{C}_{1-x}) - x\mu_{\text{Ti}} - (1-x)\mu_{\text{C}} \quad (1)$$

where  $E_{\text{coh}}(x)$  is the cohesive energy of the system,  $\mu_{\text{Ti}}$  and  $\mu_{\text{C}}$  are the chemical potentials of the Ti and C atoms, respectively. The relative stability of different Ti<sub>x</sub>C<sub>1-x</sub> structures can be gauged by comparing their  $\delta F$ : higher  $\delta F$  means inferior stability. We here set  $\mu_{\text{C}}$  and  $\mu_{\text{Ti}}$  as the cohesive

energy of graphene and bulk *hcp* Ti. The results are summarized in Figure S3. A line connecting the cohesive energy of graphene and bulk Ti is used to estimate the stability of a Ti-C compound: a structure with cohesive energy below the line ( $\delta F \leq 0$ ) is stable against decomposing into graphene and Ti; when  $\delta F > 0$ , the structure becomes metastable or even unstable. The recently predicted single-layer t-TiC<sup>1</sup> has a positive  $\delta F$  and hence is metastable. In contrast, the TiC<sub>2</sub> structure in our work has a negative  $\delta F$ , -0.40 eV, indicating a thermodynamically stability. The experimentally identified bulk TiC and 2D MXene (Ti<sub>3</sub>C<sub>2</sub> and Ti<sub>2</sub>C) also have negative  $\delta F$ . One should note that some Ti-C clusters, even though with positive  $\delta F$ , have been experimentally synthesized.<sup>2,3</sup> Therefore, the single-layer TiC<sub>2</sub> is thermodynamically favorable and may be formed when suitable synthetic conditions are provided.

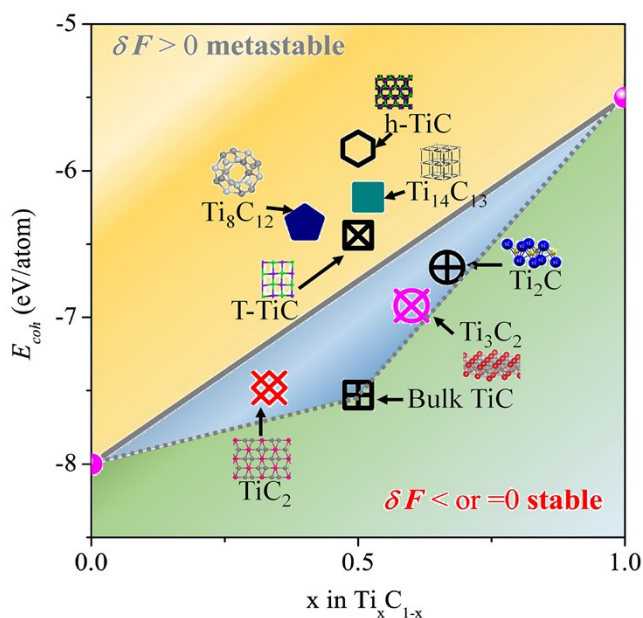


**Fig. S3** Cohesive energy for binary compounds with composition  $\text{Ti}_x\text{C}_{1-x}$ . The solid line links cohesive energies of graphene ( $x = 0$ ) and bulk Ti ( $x = 1$ ). Formation energy  $\delta F$  is positive (negative) above (below) the solid line.

#### 4. Stability relative to other isostructural metal carbides

We replace the Ti atoms in  $\text{TiC}_2$  sheet with other 3d transition metal atoms forming a series of 2D  $\text{MC}_2$  metal carbides. All structures are fully relaxed, and their cohesive energy are calculated as presented in Figure S4, which shows that  $\text{TiC}_2$  has the largest cohesive energy, indicating Ti atoms bind most strongly with  $\text{C}_2$  dimers in such structure.

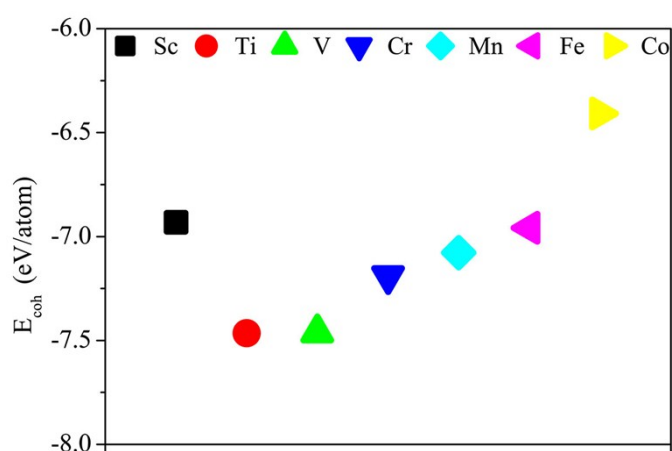


**Fig. S4** Cohesive energy of 2D transition metal dicarbides  $\text{MC}_2$  (M=Sc-Co) in the  $\text{TiC}_2$  structure.

#### 5. Thermal stability of the $\text{TiC}_2$ sheet

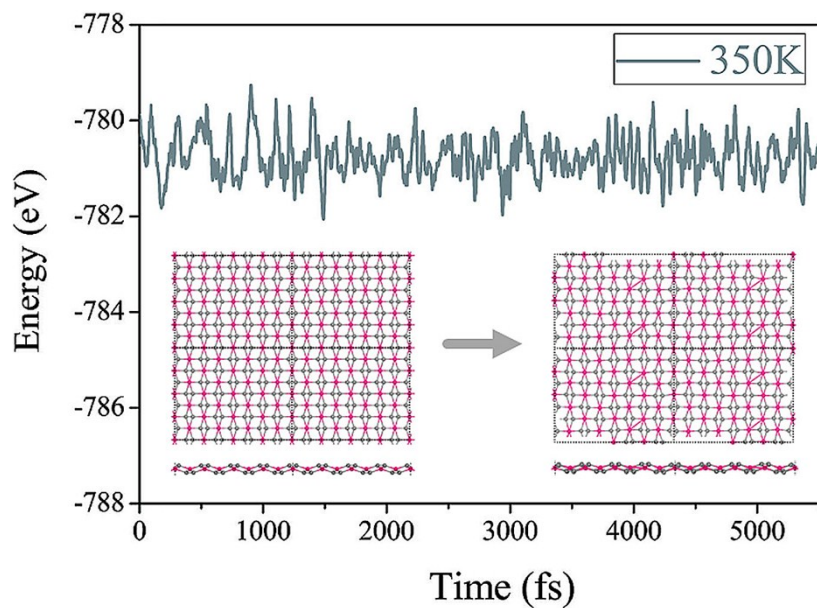


**Fig. S5** Evolution of potential energy of  $\text{TiC}_2$  during AIMD simulations at 350 K.  $4 \times 4 \times 1$  supercell is used to reduce the constraint of periodic condition in the axial direction. The insets show snapshots of atomic configurations at the beginning and the end of the simulations.

## 6. Electronic Properties of the $\text{TiC}_2$ sheet

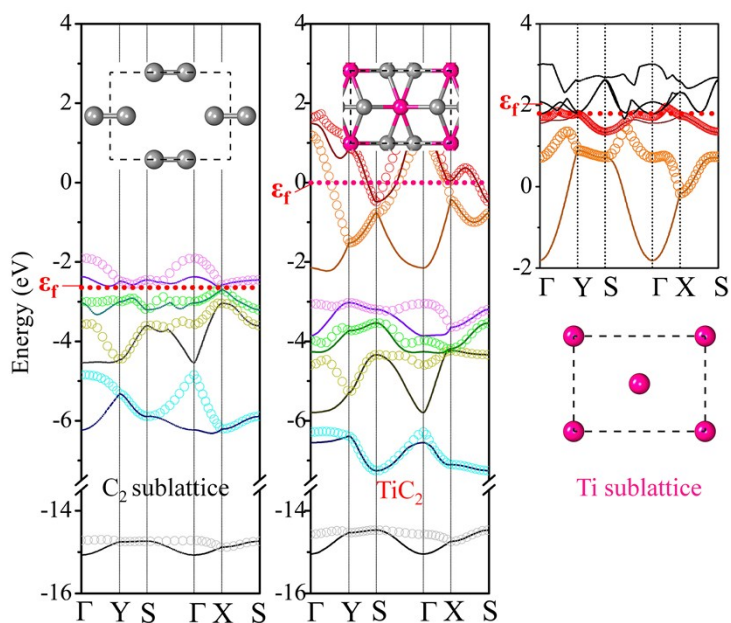


**Fig. S6** Band structure of the  $\text{TiC}_2$  sheet (center panel), the  $\text{C}_2$  sublattice (left panel), and Ti sublattice (right panel). The high symmetric k point path is along  $\Gamma (0, 0, 0) \rightarrow Y (0, 1/2, 0) \rightarrow$

$S (1/2, 1/2, 0) \rightarrow \Gamma (0, 0, 0) \rightarrow X (1/2, 0, 0) \rightarrow S (1/2, 1/2, 0)$ , corresponding to the axial direction in the real space.

### 7. Application of the $\text{TiC}_2$ sheet as Li ion battery anode material

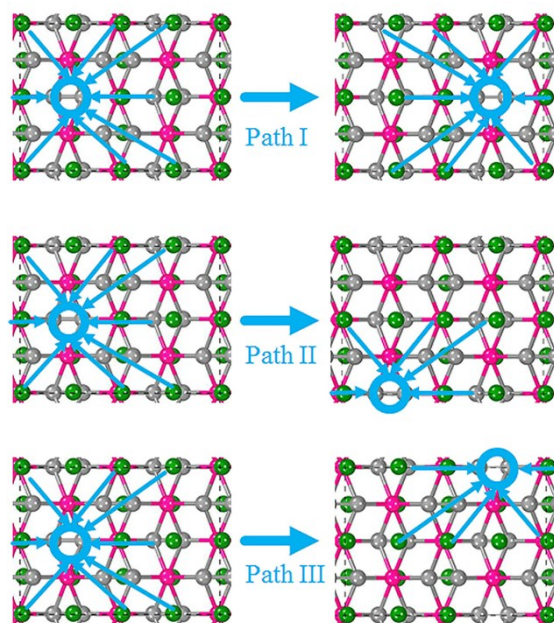


**Fig. S7** Considered migration paths of a Li “monovacancy” on the  $\text{TiC}_2$  sheet with the high coverage of  $\text{TiC}_2\text{Li}_2$ .

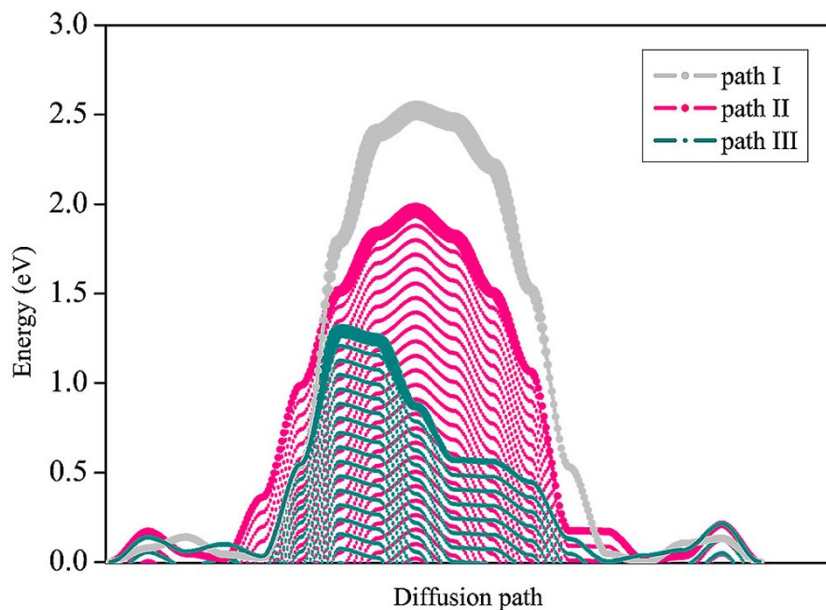
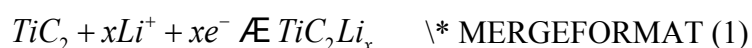


**Fig. S8** The energy barrier profiles of Li diffusion on  $TiC_2$  with the high coverage of  $TiC_2Li_2$ . The diffusion paths have been indicated in Figure S7.

#### Calculation Details: Estimation of the open circuit voltage (OCV)

Typically, the anode charge/discharge processes assume the following half-cell reaction that involves  $Li/Li^+$ :



The (OCV) for an intercalation reaction involving  $x Li^+$  ions is computed from the energy difference of the products and the reactants.

The electronic potential during this process can be written in the form of Gibbs free energy:

$$V = -\Delta G_f / zF \quad \backslash * \text{MERGEFORMAT (2)}$$

where  $z$  and  $F$  are the number of valence electrons during the adatom process and the Faraday constant, respectively;  $\Delta G_f$  is the change in Gibbs free energy during the adatom

process which is defined as:

$$\Delta G_f = \Delta E_f + P\Delta V_f - T\Delta S_f \quad \text{\* MERGEFORMAT (3)}$$

$P\Delta V_f$  is on the order of  $10^{-5}$  eV and the term  $T\Delta S_f$  is comparable to 26 meV at low temperature.<sup>4,5</sup> Thus, the entropy (thermal) effects and pressure terms are negligible, and will not be discussed further.  $\Delta G_f$  is then approximately equal to the formation energy,  $\Delta E_f$ , involved in the adsorption process, which is defined as:

$$\Delta E_f = E(\text{TiC}_2\text{Li}_x) - E(\text{TiC}_2) - xE(\text{Li}) \quad \text{\* MERGEFORMAT (4)}$$

Here  $E(\text{TiC}_2)$  denotes the total energy of pristine  $\text{TiC}_2$  monolayer,  $E(\text{Li})$  and  $E(\text{TiC}_2\text{Li}_x)$  are the total energy of bulk bcc Li and the lithiated  $\text{TiC}_2$  sheet ( $x$  Li atoms adsorbed in one supercell), respectively. The OCV is related to the formation energy by:

$$OCV = \Delta G_f / x \approx \Delta E_f / x = [E(\text{TiC}_2) + xE(\text{Li}) - E(\text{TiC}_2\text{Li}_x)] / x \quad \text{\*}$$

MERGEFORMAT (5)

## References

1. Z. Zhang, X. Liu, B. I. Yakobson and W. Guo, *J. Am. Chem. Soc.*, 2012, **134**, 19326- 19329.
2. B. C. Guo, K. P. Kerns and A. W. Castleman, *Science*, 1992, **255**, 1411-1413.
3. J.S.Pilgrim and M.A.Duncan, *J. Am. Chem. Soc.*, 1993, **115**, 9724-9727.
4. M. K. Aydinol, A. F. Kohan, G. Ceder, K. Cho and J. Joannopoulos, *Phys. Rev. B*, 1997, **56**, 1354-1365.
5. A. Van der Ven, M. K. Aydinol, G. Ceder, G. Kresse and J. Hafner, *Phys. Rev. B*, 1998, **58**, 2975-2987.